Study of the Chlorfenvinphos pesticide removal under different anodic materials and different reactor configuration

J. Mora-Gómez[a], S. Escribá-Jiménez[a], J. Carrillo-Abad[a], M. García-Gabaldón[a*], M. T. Montañés[a], S. Mestre[b], V. Pérez-Herranz[a]

[a]IEC Group, ISIRYM, Universitat Politècnica de València, Camí de Vera s/n, 46022, València, P.O. Box 22012, E-46071, Spain

[b]Instituto Universitario de Tecnología Cerámica, Universitat Jaume I, Castellón, Spain.

*Corresponding author: mongarga@iqn.upv.es

Abstract

The present manuscript focuses on the study of the electrochemical oxidation of the insecticide Chlorfenvinphos (CVP). The assays were carried out under galvanostatic conditions using boron-doped diamond (BDD) and low-cost tin dioxide doped with antimony (Sb-doped SnO_2) as anodes. The influence of the operating variables, such as applied current density, presence or absence of a cation-exchange membrane and concentration of supporting electrolyte, was discussed. The results revealed that the higher applied current density the higher degradation and mineralization of the insecticide for both anodes. The presence of the membrane and the highest concentration of Na_2SO_4 studied (0.1 M) as a supporting electrolyte benefited the oxidation process of CVP using the BDD

electrode, while with the ceramic anode the elimination of CVP was lower under these experimental conditions. Although the BDD electrode showed the best performance, ceramic anodes appear as an interesting alternative as they were able to degrade CVP completely for the highest applied current density values. Toxicity tests revealed that the initial solution of CVP was more toxic than the samples treated with the ceramic electrode, while using the BDD electrode the toxicity of the sample increased.

Keywords: BDD anode, Chlorfenvinphos, electrochemical oxidation, Sb-doped SnO_2 ceramic anode.

1. Introduction

In the last century, the rapid increase in the world population has caused a growing demand for food. For this reason, chemical substances have been used in both agriculture and farming, among these chemicals organophosphate pesticides are found (Baken et al., 2018). The indiscriminate use of these compounds cause water pollution due to the lack of technologies capable of eliminating them (Oliveira et al., 2014).

Chlorfenvinphos (CVP), 2-chloro-1 vinyl diethyl phosphate, whose structure is shown in Figure 1 of the Supplementary Material, is used against pests of ectoparasitic insects, such as mosquitoes, sandflies, tsetse flies, blackflies, tabanids, etc. This pesticide is not only used in farming and agriculture but also to fight domestic pests (Dorsey and Kueberuwa, 1997). Consequently, CVP can be found in both domestic wastewater and natural water bodies (Barco-Bonilla et al., 2013).

CVP is of artificial origin, that is, it is not generated naturally in the environment. Furthermore, this compound is hazardous for human health due to its neurotoxicity (Rickwood and Galloway, 2004). It acts as an inhibitor of the acetylcholinesterase enzyme, causing overstimulation of cholinergic neurotransmission, producing symptoms such as increased salivation, changes in blood pressure and heart rate, nausea, headache, muscle tremor, paralysis and even death (Acero et al., 2008). Due to its high toxicity, this compound has been banned in the European Union. It is also part of the list of 33 priority substances in the field of water policy approved in Decision 2455/2001/EC of the European Parlament and of the Council of 20 November 2001. In the United

States its use has been prohibited since 1991, as it was considered an extremely dangerous substance. On the other hand, in other countries such as Australia, it has been used until a few years ago (Szatkowska et al., 2012). In Kenya, a decade ago, CVP became the most widely used acaricide, which caused its presence even in cow's milk (Kituyi et al., 1997). Recent studies carried out in Spain confirmed CVP presence in honeybees, pollen and in their hive. In this last matrix, it was detected in 95% of the cases studied (Calatayud-Vernich et al., 2018). This insecticide causes the bees to become disoriented and unable to carry out pollination. This fact shows that CVP is still present in the environment despite its use was prohibited years ago. Therefore, it is necessary to develop an effective technique able to eliminate CVP presence in the environment.

Various authors have focused their research on the study of CVP degradation through techniques such as ozonation (Acero et al., 2008); adsorption (Rojas et al., 2015); Fenton and photo-Fenton (Gromboni et al., 2007; Oliveira et al., 2014; Ruíz-Delgado et al., 2019); and photoelectrocatalysis (Roselló-Márquez et al., 2019). This paper proposes the electrochemical advanced oxidation processes (EAOPs) for the elimination of this insecticide. This technique is very effective in removing emerging contaminants and refractory compounds from wastewater (Domínguez et al., 2012; Garcia-Segura et al., 2018; Martínez-Huitle et al., 2015), even for low concentrations. Moreover, EAOPs do not require the addition of chemicals and, generally, do not generate sludge either, so this method belongs to the category of clean technology (Forero et al., 2005).

EAOPs are based on the formation of hydroxyl radicals on the anodic surface through the oxidation of water (Equations 1 and 2).

$$M + H_2O \rightarrow M(^{\bullet}OH) + H^+ + e^- \quad (1)$$

$$M(^{\bullet}OH) + R \rightarrow M + R_{ox} + H^+ + e^- \quad (2)$$

where *M* is the anodic surface, M(•OH) are the hydroxyl radicals adsorbed on the anodic surface, *R* and R_{ox} is the contaminant in its initial and oxidized form, respectively. Hydroxyl radicals are capable of oxidizing most organic compounds to carbon dioxide (CO_2) and water (Moreira et al., 2017). The short life of these oxidants (Del Greco and Kaufman, 1962) explains why they are not present in the treated water.

EAOPs depend on the nature of the anode material. The complete mineralization of organic refractory compounds to CO_2 is only achieved for anodes with high oxygen overvoltage because the generation of •OH radicals destined for the oxidation of pollutants on the anodic surface is greater (Comninellis and Chen, 2010; Hmani et al., 2009). One well known material is the BDD electrode widely used on a laboratory scale in EAOPs because this material presents a wide potential window, high chemical and mechanical stability and long life (Liu et al., 2009; Oturan et al., 2013), but its high cost and the need to find a suitable substrate do not make it viable for an industrial scale (Chaplin, 2014). Anodes based on SnO_2 also poses a high oxygen overpotential (Comninellis and Chen, 2010; Wang et al., 2016), however, they usually present low stability under anodic polarization (Lipp and Pletcher, 1997).This problem has been solved by developing SnO_2 electrodes on a low-cost ceramic substrate (Droguett et al., 2020; Mora-Gómez et al., 2020), so these ceramic electrodes become very attractive for EAOPs. Additionally, these ceramic electrodes have shown acceptable degradation and mineralization results for other organic compounds,

becoming a suitable alternative to BDD anodes (Carrillo-Abad et al., 2020a, 2020b; Droguett et al., 2020; Mora-Gómez et al., 2020, 2019, 2018).

The objective of this paper is to study the influence of different variables such as the anodic material (BDD or ceramic electrode based on SnO_2), applied current density, reactor configuration (absence or presence of a cation-exchange membrane) and concentration of supporting electrolyte on the electro-oxidation of Chlorfenvinphos and on the toxicity of the treated solutions.

2. Experimental

2.1 Electrochemical oxidation assays

Electrolysis experiments were carried out galvanostatically in an undivided cell at applied current densities values (i) between 17 and 83 mA cm^{-2} using a power supply (Peaktech® 1585) during 4 hours. The solution to be treated consisted of 250 cm^3 of 60 ppm of CVP (Sigma-Aldrich) in 0.014 M of Na_2SO_4 as supporting electrolyte. Two different materials were used as anodes: a microporous Sb-doped SnO_2 ceramic electrode, described in previous studies (Mora-Gómez et al., 2020, 2019, 2018), and a Boron-doped diamond (BDD) electrode (NeoCoat SA, Switzerland). The area of both anodes was 12 cm^2. As cathode and reference electrodes were used an AISI 304 stainless steel sheet of 20 cm^2, and an Ag/AgCl one, respectively.

Electro-oxidation tests were also performed in a divided reactor by a cation-exchange membrane (Nafion 117 from Dupont). In this reactor, the solution to be treated containing the insecticide (60 mg L^{-1} of CVP and 0.014 M of Na_2SO_4) was

132 introduced in the anodic compartment and a solution with the same concentration
133 of supporting electrolyte without CVP was put in the cathodic compartment.

134 The effect of the concentration of the supporting electrolyte was also studied
135 under this reactor configuration. For this purpose, electrochemical tests were
136 carried out with different concentrations of Na_2SO_4: 0.014, 0.05 and 0.1 M.
137
138 *2.2 Analytical methods*

139 *2.2.1 Analysis of Chlorfenvinphos degradation*

140 The evolution of CVP concentration was monitored by measuring its absorbance
141 using a UV/Vis double beam spectrophotometer, model Unicam UV4-200 (Pye
142 Unicam, Cambridge). The UV/VIS spectra of CVP presents two characteristic
143 absorption bands, specifically at 205 and 244 nm. The band placed at 244 nm
144 was the one selected to follow the evolution of the CVP concentration, since the
145 first band presented a very low coefficient of linearity with the concentration
146 (Acero et al., 2008). This second absorption band is related to the electronic
147 transition π→π* of the aromatic ring (Fernández-Domene et al., 2019).

148 The measurement of Total Organic Carbon (TOC) was carried out through a
149 Shimadzu TNM-L ROHS TOC analyser. The relationship between the partial and
150 total mineralization of the compound is analysed by the extent of the
151 electrochemical combustion parameter (Φ) defined in Equation 3.
152

$$\emptyset(t) = \frac{\%[TOC(t)]_{removed}}{\%[CVP(t)]_{removed}} \quad (3)$$

153

The mineralization current efficiency (MCE) represents the fraction between the amount of organic matter removed and the amount of theoretical organic matter removed considering that the applied electrical charge is used only for the mineralization of the organic contaminant for a given instant of time. The MCE is calculated through Equation 4 (Özcan and Özcan, 2018):

$$MCE(\%) = \frac{nFV\Delta[TOC]_t}{7.2\text{x}10^5 mIt} x100 \quad (4)$$

where $\Delta[TOC]_t$ (mg L^{-1}) is the TOC removal after a certain time, t(min), F is the Faraday constant (96485 C mol^{-1}), n is the number of exchanged electrons in the oxidation reaction of CVP (56 according to reaction 5), V is the volume of the electrolytic cell (L), m is the number of carbon atoms in the CVP molecule (12), I the applied current (A) and $7.2x10^5$ is a conversion factor (60 s min^{-1} x 12000 mg mol^{-1}). Based on the molecular formula and the literature (Klamerth et al., 2009), the total mineralization reaction for CVP could be expressed as follows:

$$C_{12}H_{14}Cl_3O_4P + 24H_20 \rightarrow 12CO_2 + 3Cl^- + PO_4^{3-} + 62H^+ + 56e^- \quad (5)$$

2.2.2 Determination of oxidizing species

During the electrochemical oxidation process, in addition to the •OH radicals (Equation 1), the supporting electrolyte can also be oxidized and give rise to different oxidizing species depending on its composition. Furthermore, H_2O_2 can also be formed from the decomposition of •OH radicals. Considering that Na_2SO_4

is the supporting electrolyte employed, the oxidation reactions involved are (de Araújo et al., 2018; Murugananthan et al., 2011; Zhang et al., 2015):

$$2(^{\bullet}OH) \rightarrow H_2O_2 \quad (6)$$

$$2SO_4^{2-} \rightarrow S_2O_8^{2-} + 2e^- \quad (7)$$

$$SO_4^{2-} + {}^{\bullet}OH \rightarrow SO_4^{-\bullet} + OH^- \quad (8)$$

$$2SO_4^{-\bullet} \rightarrow S_2O_8^{2-} \quad (9)$$

The determination of the $S_2O_8^{2-}$ and H_2O_2 species was carried out by iodometry and UV spectrophotometry (Mora-Gómez et al., 2020). The amount of $^{\bullet}OH$ and $SO_4^{-\bullet}$ radicals cannot be determined using these techniques due to their short lifetime (Del Greco and Kaufman, 1962; Olmez-Hanci and Arslan-Alaton, 2013; Roots and Okada, 1975).

2.2.3 Toxicity measurements

The oxidation processes of organic matter can lead to more toxic by-products than the initial compound (Heberle et al., 2017; Oturan et al., 2008). For this reason, ecotoxicity tests have been carried out using Microtox® bioassay. This method consisted of measuring the reduction in bioluminescence of the *Vibrio Fischeri* bacterium after 15 minutes of exposure. The bioluminescence study or Microtox® bioassay (standard method UNE-EN ISO 11348-3) was carried out with the Microtox M-500 equipment (Microbics, 1989).

The tests were carried out at 15ºC, a salinity level of 2% NaCl and a pH in the 6 to 8 range. Toxicity can be expressed as n-TU (toxicity units), where n is the

number of times that a sample has to be diluted in order to inhibit the luminescence of 50% of the luminescent microorganisms. This parameter is related to the EC_{50} one, which is defined as the effective nominal concentration of a toxicant (mg L^{-1}) that reduces the intensity of light emission by 50%.

3. Results and discussion

3.1 Effect of applied current density

Figure 1 shows the variation of the CVP relative concentration as a function of time for the two electrodes under study. As can be seen, as the current density increased, the removal of the CVP was greater using both anodes. Regarding the anode material, less degradation of the CVP was achieved using the ceramic electrode with respect to the BDD one, and this difference was greater as the current density increased. This is due to the fact that the BDD electrode presents a higher overpotential for the formation of O_2 than the ceramic electrode, as observed in a previous study (Mora-Gómez et al., 2018). Therefore, a greater amount of $^{\bullet}OH$ radicals are generated in the BDD electrode. In addition, the interaction of these radicals with the surface of the BDD electrode is weaker than with the ceramic electrode (Chen et al., 2005).

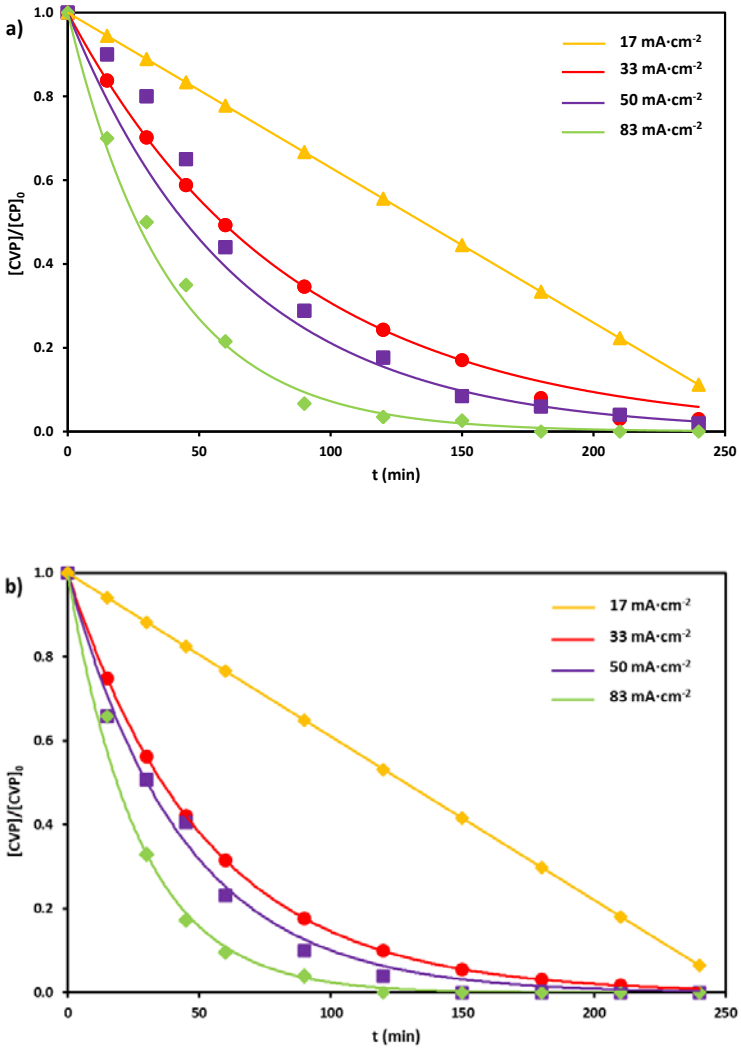

214 **Figure 1.** Effect of the applied current density on the decay of the
215 Chlorfenvinphos (CVP) relative concentration as a function of time for the ceramic
216 electrode (a) and BDD electrode (b).

217

218 In Figure 1 is also observed that when the applied current density is 17 mA cm^{-2},
219 the evolution of the relative concentration of CVP decreased linearly with time for
220 both anodes. This behaviour is typical of an electrochemical system controlled by
221 charge transfer (Li et al., 2008), that is, the velocity of •OH radicals generation on
222 the anodic surface is lower than the transport rate of the CVP molecules to the
223 anode, because the solution is fully stirred; and also than the chemical oxidation

224 reaction of CVP. Therefore, the rate of the degradation process is independent
225 of the concentration of the compound to be oxidized (Equation 10)
226 (Chatzisymeon et al., 2009).
227

$$r_{(R)} = V\frac{d[R]}{dt} = -V\frac{d[^{\bullet}OH]}{dt} = -\frac{I\theta}{nF} \quad (10)$$

228

229 where **θ** represents the current efficiency related to the •OH radical generation.

230 In this case, for a constant current density, the system can be fitted to a pseudo-
231 zero order kinetics (Equation 11), and the kinetic constant (k_0) is calculated with
232 Equation 12. The values obtained for k_0 are 0.208 and 0.210 mg L^{-1} for the
233 ceramic and BDD electrodes, respectively. This indicates that for low current
234 values, the CVP degradation rate is very similar using both anodes.
235

$$\frac{d[CVP]}{dt} = -\frac{I\theta}{nFV} = -k_0 \quad (11)$$

$$[CVP]_t = [CVP]_0 - k_0 \cdot t \quad (12)$$

236

237 However, from 33 to 83 mA·cm^{-2}, the evolution of the relative concentration of
238 CVP with time followed an exponential trend, as predicted by Equation (14).
239 Assuming that the system was perfectly stirred, this trend indicates that the
240 process was controlled by the oxidation reaction of CVP by •OH radicals, as
241 observed in other studies (Mora-Gómez et al., 2020, 2019). In this case, the
242 velocity of the CVP electro-oxidation reaction can be written according to
243 Equation (13):

$$\frac{d[CVP]}{dt} = -k[CVP][\cdot OH] = -k_{app}[CVP] \quad (13)$$

where k is the kinetic constant. For a given current density, the concentration of hydroxyl radicals is constant, and an apparent pseudo-first order constant (k_{app}) can be defined. This parameter can be calculated by integrating the previous equation, Equation 14 (Mora-Gómez et al., 2020).:

$$[CVP]_t = [CVP]_0 e^{-k_{app}t} \quad (14)$$

The k_{app} values obtained for both anodes as a function of the current density are represented in Figure 2 of the Supplementary Material. The velocity of CVP removal with the BDD electrode was higher than that obtained with the ceramic one, since in the BDD electrode the formation of active radicals is greater, as already mentioned. Regarding the current density effect on the kinetics, when i increased the k_{app} was also increased, and this increase is proportional to i for both electrodes. This can be explained by the proportional increase in the formation of active oxidant species, that react with CVP, as a function of the applied current.

The apparent kinetic constants calculated for both anode materials and for all the applied current values were used to calculate the theoretical decay of the CVP concentration predicted by Equation 14. In Figure 1a and 1b is also presented the comparison of the data (as dots) together with the theoretical values (continuous lines), where a good fitting is observed for all the conditions studied.

The evolution of the relative concentration of TOC with the electrolysis time for the previous conditions is shown in Figure 2. For an electrolysis time of 150 min, with the ceramic electrode, mineralization values of 49.6%, 62%, 70% and 75.4% were reached applying current densities of 17, 33, 50 and 83 mA cm^{-2}, respectively. Under the same experimental conditions, the TOC decay obtained for the BDD one was of 58%, 68.3%, 78% and 80%. These results demonstrate the great oxidizing power of the BDD electrode to mineralize CVP and the rest of organic matter accumulated in solution to CO_2. As was observed for CVP removal, increasing current density caused the increase in the mineralization rate. However, complete mineralization was not achieved for these experimental conditions, so organic matter continued present in solution even though CVP was completely degraded. This fact suggests the presence of short chain carboxylic acids, as also occurred in the mineralization of other organic contaminants (Coledam et al., 2016; Özcan et al., 2016). Klamerth et al., obtained similar results of TOC mineralization when studied the CVP degradation by a photo-fenton process, which was attributed to the presence of short-chain organic acids such as maleate, acetate and pyruvanate formed at the end of the process (Klamerth et al., 2009).

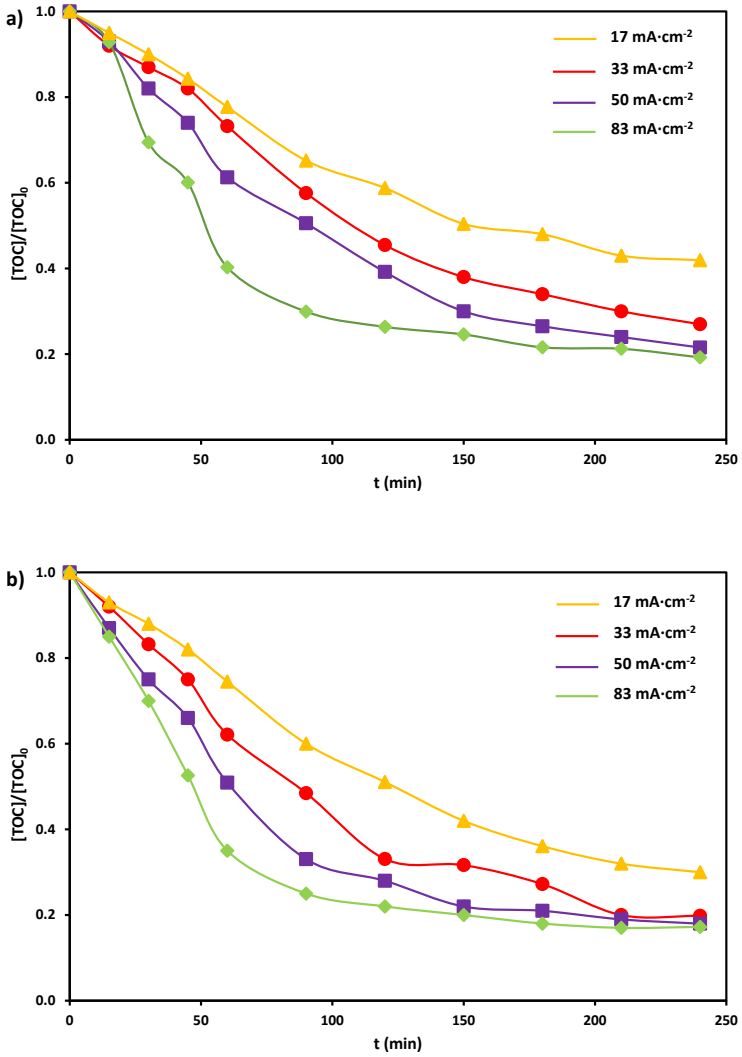

283 **Figure 2.** Effect of the applied current density on the decay of the relative total
284 organic carbon (TOC) concentration as a function of time for the ceramic
285 electrode (a) and BDD electrode (b).

286 Comparing the CVP degradation and its mineralization (Figures 1 and 2), it is
287 concluded that the degradation rate of this insecticide was greater than its
288 mineralization for both types of electrodes. This difference can be quantified by
289 the extent of electrochemical combustion (ϕ) defined in Equation 3.

290 Figure 3a presents the ϕ values obtained as a function of the electrolysis time.
291 As can be seen, when the system was limited by the charge transfer process (17

292 mA cm^{-2}), initial values of ϕ were equal to or close to unity, so the CVP removed
293 was directly mineralized to CO_2. Subsequently, the values of ϕ decreased with
294 the electrolysis time, being slightly higher with the BDD electrode. When the
295 system was limited by the oxidation reaction of the CVP (50 mA cm^{-2}), it can be
296 observed that ϕ was less than unity and it increased with the electrolysis time.
297 This increase is related to the conversion of the organic by-products generated
298 to CO_2 as the electrolysis progressed. This same trend was observed for 33 and
299 83 mA·cm^{-2} (not shown), actually, the curves for these three values of applied
300 current and both anodic materials are almost overlapped. This behaviour is
301 similar to that observed for other emerging contaminants under the same
302 conditions (Mora-Gómez et al., 2020, 2019). On the other hand, for CVP, there
303 was not a clear trend of ϕ values regarding the type of anode.

304 With respect to MCE, its evolution as a function of time for both electrodes is
305 depicted in Figure 3b; this parameter decreased with time since the organic
306 matter present in solution also decreased. Furthermore, this downward effect was
307 more pronounced for the lowest current density. Using the ceramic electrode, the
308 average MCE values reached were 6.1%, 3.22%, 3.1% and 2.83% for the current
309 densities of 17, 33, 50, and 83 mA cm^{-2}, respectively, while with the BDD
310 electrode for the same assay conditions, average MCE values of 6.74%, 3.97%,
311 3.31% and 2.84% were obtained. Therefore, this last electrode was slightly more
312 efficient than the ceramic one due to its high capacity to generate active oxidants.
313 The decrease of MCE as i increases observed for all the experimental conditions
314 can be justified by the increase in the parasitic reactions (Equations 7 to 9, 15
315 and 16).
316

$$M(^{\bullet}OH) + H_2O \rightarrow M + O_2 + 3H^+ + 3e^- \quad (15)$$

$$2M(^{\bullet}OH) \rightarrow 2M + O_2 + 2H^+ + 2e^- \quad (16)$$

317

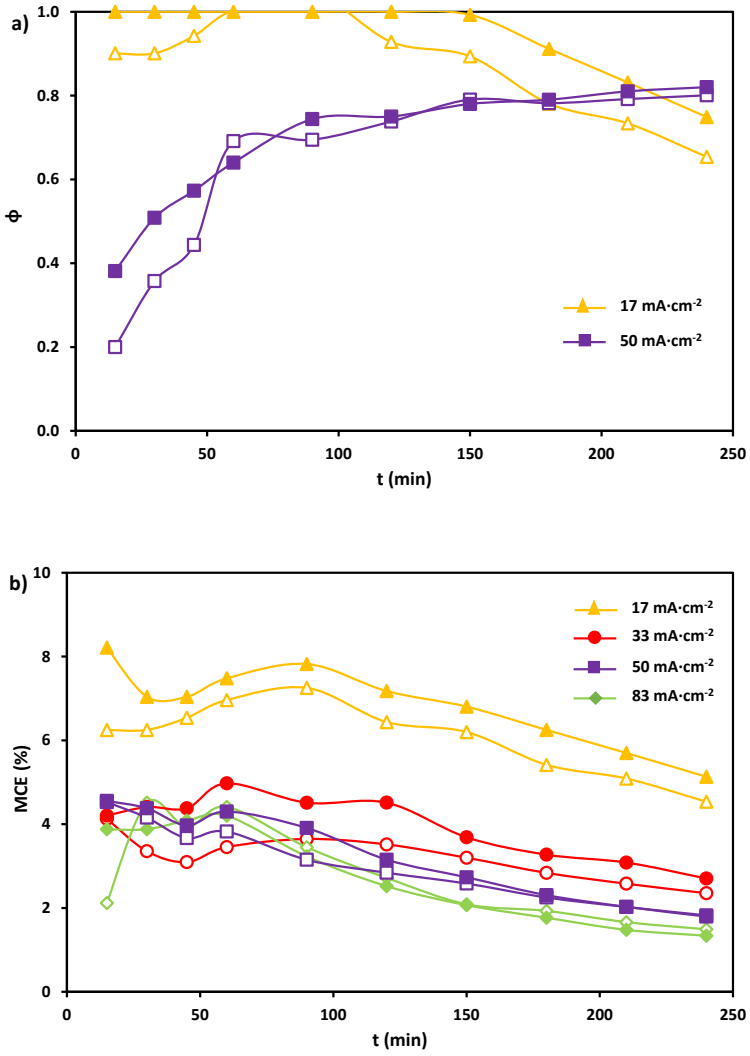

318 **Figure 3.** Effect of the applied current density on ϕ (a) and on MCE (b) as a
319 function of time. Solid points represent BDD electrode and empty points the
320 ceramic one.

321

3.2 Effect of the reactor configuration

Figure 4 shows the evolution of the relative concentration of CVP (Figure 4a) and TOC (Figure 4b) as a function of time for both electrodes in the presence of a cation-exchange membrane. Regarding the CVP removed, for an electrolysis time of 150 minutes and at 33 and 83 mA cm^{-2}, a CVP removal of 75% and 95.69% was achieved using the ceramic electrode, and a 97.91% and 100% with the BDD one, respectively. Comparing these values with those obtained in the absence of membrane (82.97% and 97.38% for the ceramic electrode, and 94.38% and 100% for the BDD), it is concluded that no improvements were observed due to the presence of the cation-exchange membrane, especially with respect to the ceramic electrode. This fact contrasts with the results observed for other studies carried out with this ceramic electrode (Mora-Gómez et al., 2020, 2019).

Regarding the mineralization of organic compounds (Figure 4b), after 150 minutes of electrolysis, in the divided reactor the mineralization values of 47% and 50.73% were reached with the ceramic electrode and 68.7% and 100% with the BDD one at 33 and 83 mA cm^{-2}, respectively, compared to 62% and 75.4% for the ceramic and 68.3% and 80% for the BDD electrode in the absence of a membrane, as previously mentioned. Hence, the use of the cation-exchange membrane worsened the mineralization of the organic matter for the ceramic electrode. This fact suggests that the intermediates formed from CVP in the membrane reactor were more persistent to the electrochemical degradation. Another explanation could be that CVP and its formed by-products with this anode in the undivided reactor could also be degraded by their reduction at the cathode, as it has previously been observed for other emerging pollutants

(Méndez-Martínez et al., 2012; Radjenović et al., 2012). On the contrary, with the BDD electrode, complete mineralization was achieved in the presence of the membrane at 83 mA cm^{-2}.

To clarify the results obtained with the ceramic electrode, an experiment was carried out in the presence of the membrane at 83 mA cm^{-2} but introducing the initial solution of CVP in the cathodic compartment. The results (Figure 3 of the Supplementary Material) showed that this insecticide was also degraded by its reduction during electrolysis as occurred with other compounds (Droguett et al., 2020; Méndez-Martínez et al., 2012; Radjenović et al., 2012). Therefore, improvements were observed in the undivided reactor with ceramic electrode. In the case of the BDD, since its oxidation power is greater, the effect of the reduction was not so evident.

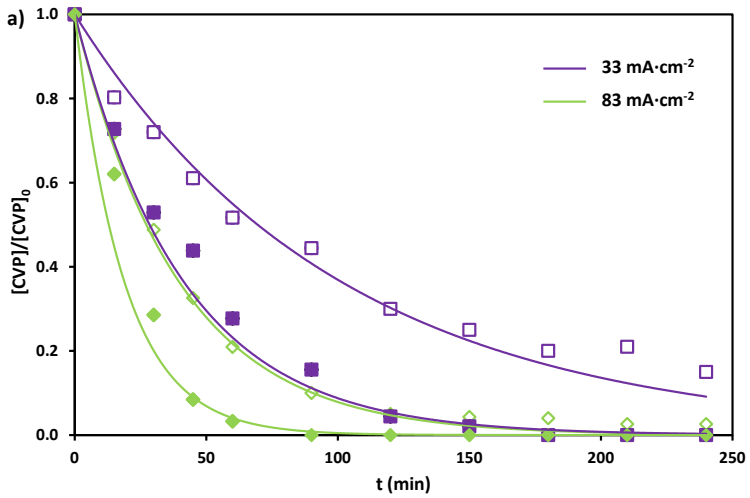

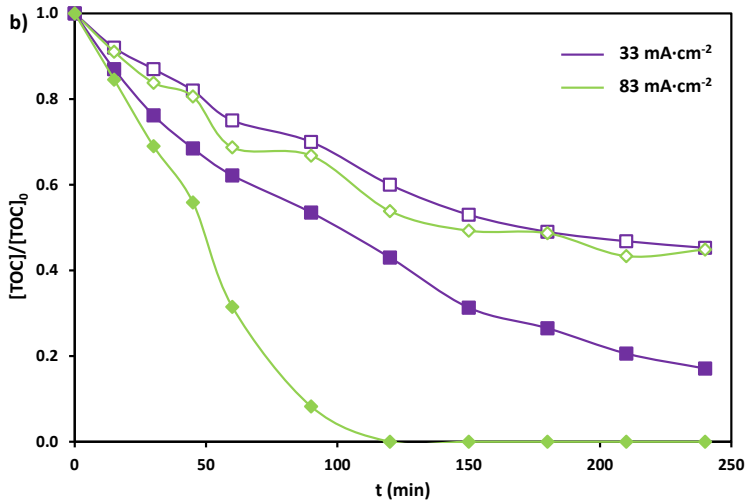

Figure 4. Effect of the applied current density on the decay of the relative CVP (a) and TOC (b) concentration as a function of time for the divided reactor. Solid points represent BDD electrode and empty points the ceramic electrode.

Regarding the electrochemical parameters of ϕ and MCE, it was concluded that the ϕ value increased with the electrolysis time and, for this reactor configuration, the obtained values of ϕ were greater with the BDD electrode because the CVP mineralization achieved was greater than with the ceramic one. However, in presence of the membrane and using the BDD electrode at 83 mA cm^{-2}, after 120 minutes of electrolysis the extent of electrochemical combustion reached the unity because all the initial CVP has been mineralized. Regarding the MCE parameter, in the presence of the membrane, the average MCE values with the ceramic electrode were 3.16% and 1.70%, and with the BDD anode were 4.94% and 2.14% at 33 and 83 mA cm^{-2}, respectively. Therefore, it was verified that for both reactor configurations an increase in the applied current density causes a decrease in the MCE.

Figure 5 and 6 presents, respectively, the comparison of the electrochemical combustion parameter and the mineralization current efficiency, for both reactor configuration and both anodic materials at two different values of applied current. Comparing the reactor configuration, both the ϕ and MCE values for the ceramic electrode were lower in the divided reactor (Figures 5a y 6a), while using the BDD anode, in the presence of a membrane the values obtained were higher since the mineralization achieved was also higher, specially at the highest applied current value. This fact can be attributed to the lower pH values reached in the anodic compartment since H^+ ions were formed during the electrochemical process, which contribute to increase the standard redox potential of hydroxyl radicals and, consequently, to increase their oxidation power [27].

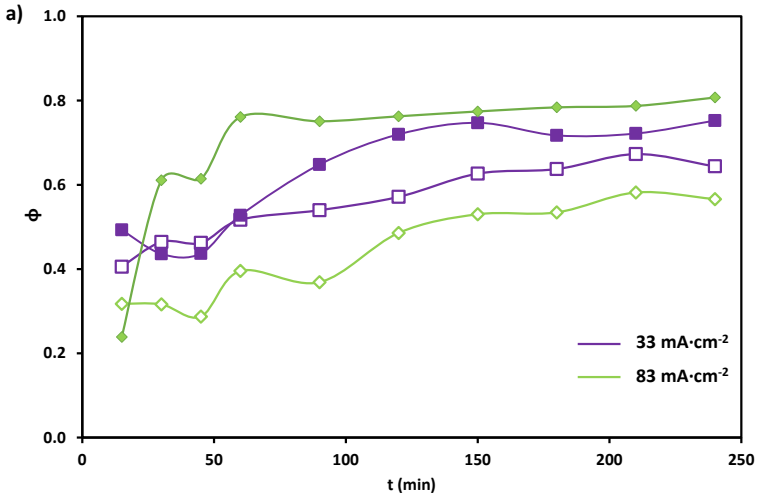

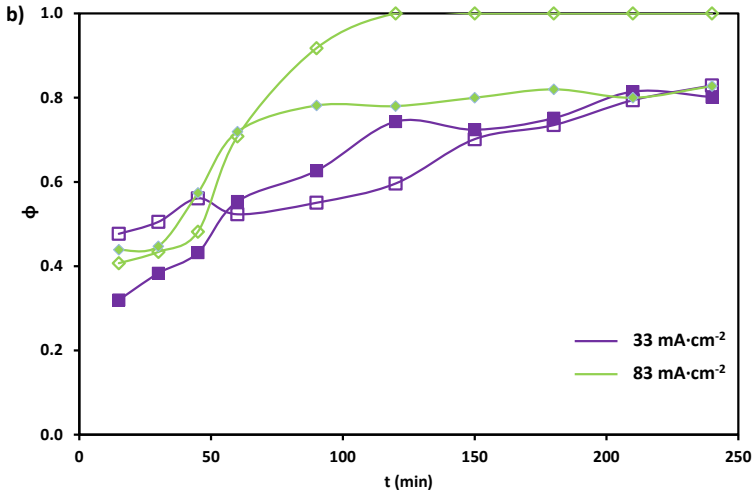

389

390

391 **Figure 5.** Evolution of **Φ** as a function of time in the presence (empty points) and

392 absence (solid points) of the cation-exchange membrane for the ceramic

393 electrode (a) and the BDD electrode (b).

394

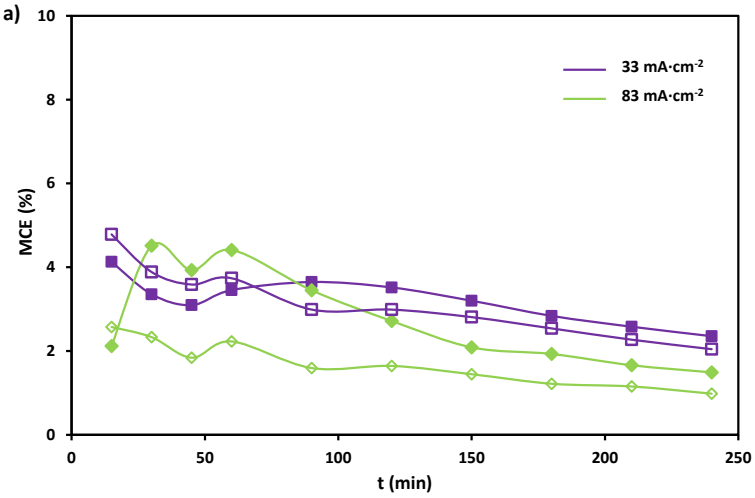

395

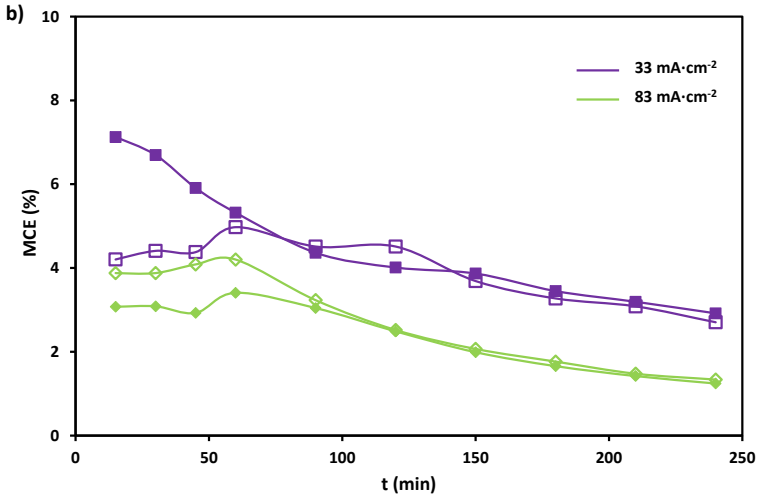

Figure 6. Evolution of MCE as a function of time in the presence (empty points) and absence (solid points) of the cation-exchange membrane for the ceramic electrode (a) and the BDD electrode (b).

Figure 4 presented in the Supplementary Material shows the evolution of the UV/VIS spectra during the electrochemical degradation of CVP for both electrodes and reactor configurations at 33 mA cm^{-2}. In this figure, it is observed that, generally, the UV/VIS spectrum decreased with time for the same assay. For the BDD electrode in the divided reactor, it can be observed that for intermediate times (between 30 and 90 minutes) in the UV/VIS spectrum a new band appeared around a wavelength of 215 nm, indicating the formation of some by-product of the CVP oxidation reaction that absorb at this wavelength. In addition, it was also observed that for these conditions (BDD in the divided reactor), from 150 minutes for wavelengths between 200 and 210 nm, the UV/VIS spectrum increased with time, so it can be indicative of increased persulfate formation, since these oxidant species absorb at a wavelength of 205 nm (An et al., 2015), in addition to the formation of short-chain carboxylic acids (Coledam et al., 2016; Özcan et al., 2016).

3.3 Effect of sodium sulfate concentration

Figure 7 shows the evolution of CVP relative concentration with time as a function of the Na_2SO_4 concentration for the applied current densities values of 33 and 83 mA cm^{-2}. In the case of the ceramic electrode (Figure 7a), the higher supporting electrolyte concentration the lower CVP degradation rate, this decrease being more notable at the lowest applied i (33 mA cm^{-2}). As already observed by other authors (Zhang et al., 2015; Zhong et al., 2013), this fact may be associated to a larger amount of sulfate ions adsorbed on the anode surface minimizing active sites and, therefore, inhibiting the electro-generation of oxidizing species, mainly $^{\bullet}OH$ radicals. For example, for Na_2SO_4 concentrations of 0.014, 0.05 and 0.1 M at 45 minutes of electrolysis, applying a current density of 33 mA cm^{-2}, a CVP removal of 41.2%, 33.6% and 32.9% was achieved, and at 83 mA·cm^{-2}, a CVP degradation rate of 65.1%, 62.4% and 61.5%, respectively. At the highest i (83 mA cm^{-2}) with this electrode, after 180 minutes of electrolysis, the CVP was completely degraded for the three concentrations of supporting electrolyte.

Using the BDD electrode (Figure 7b), under the same current densities, the increase in the concentration of the supporting electrolyte implied an improvement in the degradation of the CVP specially at 33 mA cm^{-2}. At the lowest i, after 45 minutes of assay, the CVP has been removed by 57.9%, 59.1% and 66.9% for 0.014, 0.05 and 0.1 M of Na_2SO_4 concentrations, respectively. On the other hand, for the highest i, the CVP removed was 82.6%, 84.7% and 85.15%, respectively. Generally, complete CVP degradation was reached at 120 minutes of electrolysis. This improvement with Na_2SO_4 concentration was attributed to the

fact that the BDD electrode, in addition to $^{\bullet}OH$ radicals (Ma et al., 2018), it produces $S_2O_8^{2-}$ and $SO_4^{-\bullet}$ by oxidation of sulfates according to Equations 7 to 9. These species present a high oxidation power (2.07 V and 2.4 V vs SHE, respectively) (Huie et al., 1991; Liang et al., 2008), so they are capable of oxidizing organic compounds. This fact also coincides with the new absorption band observed in the UV/Vis spectra at 205 nm associated with a greater formation of persulfate ions (Figure 4b of the Supplementary material).

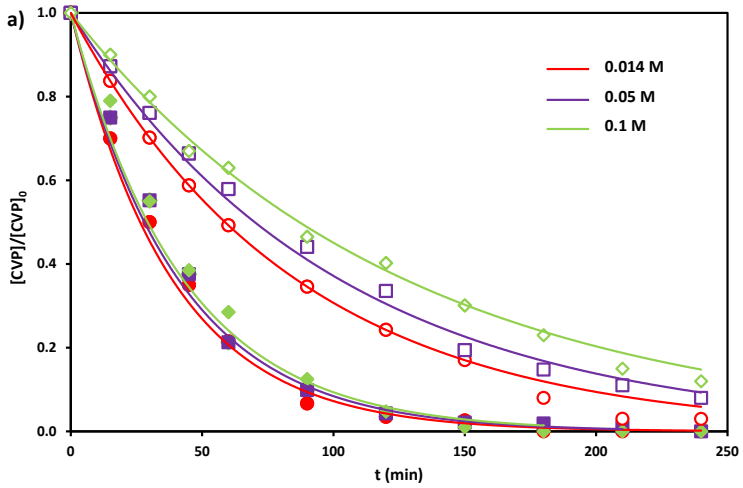

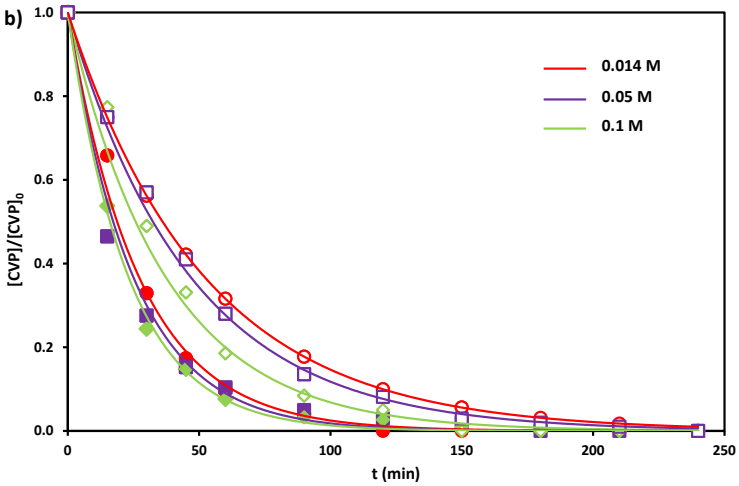

Figure 7. Effect of Na_2SO_4 concentration on the evolution of relative CVP concentration as a function of time for the ceramic electrode (a) and the BDD electrode (b). Empty points represent 33 $mA \cdot cm^{-2}$ and solid points 83 $mA \cdot cm^{-2}$.

In Figure 7, it is also observed that the relative concentration of CVP follows an exponential decay, and as the system was perfectly stirred, this is an indication of that the system was limited by the oxidation reaction of CVP. Therefore, data was fitted to a pseudo-first order system, Equation (14), and k_{app} values were calculated. In Figure 5 of the Supplementary Material, k_{app} values are represented as a function of the Na_2SO_4 concentration for the two current densities applied with both types of anodes. Using the ceramic electrode, it can be verified that the CVP degradation velocity tended to decrease with the concentration of the supporting electrolyte, as previously commented. On the contrary, with the BDD electrode for both values of i applied, the CVP degradation velocity increased with the concentration of Na_2SO_4. For both electrodes, and as previously verified with this contaminant, k_{app} increased when the applied current

density, since the generation of oxidant species, especially $^{\bullet}OH$ radicals, was also greater.

Figure 6 of the Supplementary Material shows the influence of the Na_2SO_4 concentration on the mineralization of the CVP. The trend observed for each electrode similar to that described for the CVP degradation, that is, an increase in the concentration of Na_2SO_4 caused a decrease in the velocity of the CVP mineralization process with the ceramic electrode and an increase with the BDD electrode. At the end of the electrolysis experiment, at 33 mA cm^{-2}, the CVP was mineralized by 73.0%, 67.1% and 61.9% using the ceramic electrode and by 80.2%, 83.1 and 84.8% using the BDD for Na_2SO_4 concentrations of 0.014, 0.05 and 0.1 M, respectively. On the other hand, at the highest i, the percentage of mineralization was 80.7%, 78.9% and 75.0% with the ceramic electrode and 82.8%, 90.0% and 92.5% with the BDD one, respectively.

3.4 Analysis of electrogenerated persulfates

As mentioned previously, during the CVP electrochemical oxidation process, in addition to the •OH radicals, H_2O_2 can also be formed from the decomposition of •OH radicals, together with $S_2O_8^{2-}$ and $SO_4^{-\bullet}$ due to the supporting electrolyte oxidation. With the UV spectrophotometry method, the presence of hydrogen peroxide and $SO_4^{-\bullet}$ was not detected during any of the assays carried out, so the number of total oxidants determined by iodometry was due to persulfates, since the supporting electrolyte only contained Na_2SO_4.

When the Na_2SO_4 concentration was 0.014 M, with the ceramic electrode, persulfate formation was not detected in the single compartment reactor. Nevertheless, using the BDD electrode, the presence of these persulfate ions in solution was verified for all the experimental conditions, and their concentration was higher when i increased since the oxidation rate of the supporting electrolyte was higher. Regarding the reactor configuration, the membrane avoided the reduction at the cathode of these persulfate ions, therefore, the concentration of persulfate ions was higher in this reactor for both electrodes. With the BDD electrode, the use of the membrane caused an increase in the persulfate concentration in the anolyte of the order of 5 and 20 times with respect to the reactor in absence of membrane for both applied currents. However, the $S_2O_8^{2-}$ ions present in solution using the ceramic electrode in the anodic compartment were 10 times lower. These results agree with the evolution of UV/VIS spectra (Figure 4 of the Supplementary Material) where the appearance of an absorbance band near to 200 nm observed was associated to the presence of $S_2O_8^{2-}$ ions in presence of the membrane and using the BDD electrode.

Regarding the effect of the Na_2SO_4 concentration, the higher the concentration of the supporting electrolyte, the greater the concentration of $S_2O_8^{2-}$ ions detected in solution for both anodes (Figure 7 of the Supplementary Material). Comparing both types of anodes, it is observed again that the BDD electrode produced more persulfate ions. In addition, the formation of $S_2O_8^{2-}$ ions with the ceramic electrode only was observed for Na_2SO_4 concentrations of 0.05 and 0.1 M.

3.4 Analysis of toxicity with Vibrio Fischeri

511 Finally, toxicity measurements were carried out for the CVP degradation tests
512 using the *Vibrio Fischeri* method. The values of toxicity units (TU) of the initial
513 CVP solutions at three different concentrations of Na_2SO_4 (0.014, 0.05 and 0.1
514 M) were 3, 2 and 3 TU, respectively.

515 Regarding the treated solutions, Table 1 of the Supplentary Material presents the
516 different values of TU obtained as a function of the different experimental
517 conditions. It was observed that with the ceramic electrode, generally, the TU
518 values were null. Therefore, in addition to remove part of the contaminant and
519 organic matter, the toxicity of the initial samples decreased. With the BDD
520 electrode, in most of the treated samples, the TU values were non-zero and
521 higher than TU values of initial solutions, mainly when i and the Na_2SO_4
522 concentration increased, and in the presence of a membrane. Comparing this
523 fact with the concentrations of electrogenerated persulfates, it is verified that
524 these two measurements are related to each other, since the higher the
525 concentration of persulfates the toxicity of the sample was greater. Another
526 possibility was that phosphates and chlorides influenced in these toxicity
527 measures. However, considering that the initial concentration of CVP was 60
528 ppm, the maximum concentration of PO_4^{3-} and Cl^- that could be obtained from
529 the complete oxidation of the CVP (reaction 5) was 15.85 and 5.91 ppm,
530 respectively. However, in studies carried out using the Daphnia Magna method
531 (48 h), the EC_{50} of PO_4^{3-} and Cl^- were 1089 and 1000 ppm, respectively (Eur and
532 Kgaa, 2007a, 2007b), which are concentrations much higher than those that may
533 be present in the samples. This fact reinforces the theory that persulfates were
534 responsible for the resulting toxicity of the sample, since its EC_{50} was lower (133
535 ppm) (Eur and Kgaa, 2007c), and as observed in Figure 7 of the Supplementary

536 Material, the persulfate concentration in solution is always higher than this value
537 when using the BDD anode. Therefore, in terms of toxicity, the ceramic electrode
538 is more suitable for the electrochemical oxidation of CVP than the BDD electrode.
539

4. Conclusions

Recent studies have detected the presence in body waters of a neurotoxic insecticide, the Chlorfenvinphos (CVP). Traditional treatment methods are not adequate to treat these contaminated waters so in this work, the electrochemical advanced oxidation technique with two different anodic materials (BDD and Sb-doped SnO_2 ceramic) has been studied as an efficient method to remove this species.

This technique has been carried out in galvanostatic mode at current densities ranging from 17 to 83 $mA \cdot cm^{-2}$. For both anodes in the undivided reactor, at the lowest current density, the process is limited by charge transfer, that means, that the limiting step of the oxidation process is the velocity of generation of hydroxyl radicals ($^{\bullet}OH$). However, at higher current densities, the concentration of CVP decreases exponentially with electrolysis time since the process is limited by the chemical reaction oxidation of CVP by means of $^{\bullet}OH$ radicals.
Furthermore, when i increases, both CVP degradation and mineralization degrees are greater for both anodic materials, due to a greater generation of oxidizing species, such as $^{\bullet}OH$ radicals and persulfate ions. However, the process presents lower mineralization current efficiency (MCE).

The presence of the cation-exchange membrane benefited the oxidation process using the BDD electrode since the membrane prevented the reduction of the organic intermediates and oxidizing species formed. Nevertheless, with the ceramic electrode, the highest degrees of CVP and TOC removal were obtained in the undivided reactor, due to the contribution of the reduction reaction of CVP taking place in the absence of the membrane.

564 The Na_2SO_4 concentration as supporting electrolyte also affects the
565 electrochemical degradation process, since for the BDD electrode, a higher
566 degree of mineralization is achieved at the highest Na_2SO_4 concentration and, on
567 the contrary, for the ceramic electrode, is achieved at the lowest one. This is due
568 to the ability of each electrode to oxidize sulfate ions to persulfate and sulfate
569 radicals.

570 Concerning the analysis of the oxidizing agents generated, it is proved that the
571 sulfates ions of the supporting electrolyte are oxidized to persulfate ions,
572 however, the H_2O_2 presence was not detected. The formation of persulfate ions
573 is favoured: using the BDD electrode, due to its wide electrochemical window;
574 when the Na_2SO_4 concentration is increased, at high working current densities
575 and, in the presence of the cation exchange membrane, since it prevents the
576 reduction of these species at the cathode.

577 Therefore, the results showed that ceramic electrodes can be used as effective
578 anodes for the oxidation of CVP, since for high current densities it is possible to
579 degrade a 100% of the CVP. However, the BDD electrode is the most efficient
580 one since it generates more active oxidant species on its surface.

581 Finally, in terms of toxicity, it is shown that the samples treated with the ceramic
582 electrode show less toxicity than the initial one. On the other hand, with the BDD
583 electrode the toxicity is higher, since this parameter is attributed to the persulfate
584 ions.
585
586
587

588

589 **Acknowledgments**

590

591 The authors thank the financial support from the Ministerio de Economía y
592 Competitividad (Spain) under the project RTI2018-101341-B-C21, co-financed
593 with FEDER funds.

594

595 **References**

596 Acero, J.L., Real, F.J., Javier Benitez, F., González, A., 2008. Oxidation of
597 chlorfenvinphos in ultrapure and natural waters by ozonation and
598 photochemical processes. Water Res. 42, 3198–3206.
599 https://doi.org/10.1016/j.watres.2008.03.016
600 An, D., Westerhoff, P., Zheng, M., Wu, M., Yang, Y., Chiu, C.-A., 2015. UV-
601 activated persulfate oxidation and regeneration of NOM-Saturated granular
602 activated carbon. Water Res. 73, 304–310.
603 https://doi.org/10.1016/j.watres.2015.01.040
604 Baken, K.A., Sjerps, R.M.A., Schriks, M., van Wezel, A.P., 2018. Toxicological
605 risk assessment and prioritization of drinking water relevant contaminants
606 of emerging concern. Environ. Int. 118, 293–303.
607 https://doi.org/10.1016/j.envint.2018.05.006
608 Barco-Bonilla, N., Romero-González, R., Plaza-Bolaños, P., Martínez Vidal,
609 J.L., Castro, A.J., Martín, I., Salas, J.J., Frenich, A.G., 2013. Priority
610 organic compounds in wastewater effluents from the Mediterranean and
611 Atlantic basins of Andalusia (Spain). Environ. Sci. Process. Impacts 15,
612 2194–2203. https://doi.org/10.1039/c3em00329a
613 Calatayud-Vernich, P., Calatayud, F., Simó, E., Picó, Y., 2018. Pesticide
614 residues in honey bees, pollen and beeswax: Assessing beehive exposure.
615 Environ. Pollut. 241, 106–114. https://doi.org/10.1016/j.envpol.2018.05.062
616 Carrillo-Abad, J., Mora-Gómez, J., García-Gabaldón, M., Mestre, S., Pérez-
617 Herranz, V., 2020a. Comparison between an electrochemical reactor with
618 and without membrane for the nor oxidation using novel ceramic
619 electrodes. J. Environ. Manage. 268.

https://doi.org/10.1016/j.jenvman.2020.110710

Carrillo-Abad, J., Mora-Gómez, J., García-Gabaldón, M., Ortega, E., Mestre, S., Pérez-Herranz, V., 2020b. Effect of the CuO addition on a Sb-doped SnO2 ceramic electrode applied to the removal of Norfloxacin in chloride media by electro-oxidation. Chemosphere 249. https://doi.org/10.1016/j.chemosphere.2020.126178

Chaplin, B.P., 2014. Critical review of electrochemical advanced oxidation processes for water treatment applications. Environ. Sci. Process. Impacts 16, 1182–1203. https://doi.org/10.1039/c3em00679d

Chatzisymeon, E., Dimou, A., Mantzavinos, D., Katsaounis, A., 2009. Electrochemical oxidation of model compounds and olive mill wastewater over DSA electrodes: 1. The case of Ti/IrO2 anode. J. Hazard. Mater. 167, 268–274. https://doi.org/10.1016/J.JHAZMAT.2008.12.117

Chen, X., Gao, F., Chen, G., 2005. Comparison of Ti/BDD and Ti/SnO2-Sb2O5 electrodes for pollutant oxidation. J. Appl. Electrochem. 35, 185–191. https://doi.org/10.1007/s10800-004-6068-0

Coledam, D.A.C., Aquino, J.M., Silva, B.F., Silva, A.J., Rocha-Filho, R.C., 2016. Electrochemical mineralization of norfloxacin using distinct boron-doped diamond anodes in a filter-press reactor, with investigations of toxicity and oxidation by-products. Electrochim. Acta 213, 856–864. https://doi.org/10.1016/j.electacta.2016.08.003

Comninellis, C., Chen, G., 2010. Electrochemistry for the Environment. Springer, New York.

de Araújo, D.M., Sáez, C., Cañizares, P., Rodrigo, M.A., Martínez-Huitle, C.A., 2018. Improving the catalytic effect of peroxodisulfate and

peroxodiphosphate electrochemically generated at diamond electrode by activation with light irradiation. Chemosphere 207, 774–780. https://doi.org/10.1016/j.chemosphere.2018.05.121

Del Greco, F.P., Kaufman, F., 1962. Lifetime and reactions of OH radicals in discharge-flow systems. Discuss. Faraday Soc. 33, 128–138. https://doi.org/10.1039/DF9623300128

Domínguez, J.R., González, T., Palo, P., Sánchez-Martín, J., Rodrigo, M.A., Sáez, C., 2012. Electrochemical degradation of a real pharmaceutical effluent. Water. Air. Soil Pollut. 223, 2685–2694. https://doi.org/10.1007/s11270-011-1059-3

Dorsey, A.S., Kueberuwa, S.S., 1997. Toxicological Profile for Chlorfenvinphos. ATSDR's Toxicol. Profiles 220. https://doi.org/10.1201/9781420061888_ch148

Droguett, T., Mora-Gómez, J., García-Gabaldón, M., Ortega, E., Mestre, S., Cifuentes, G., Pérez-Herranz, V., 2020. Electrochemical Degradation of Reactive Black 5 using two-different reactor configuration. Sci. Rep. 10, 1–12. https://doi.org/10.1038/s41598-020-61501-5

Eur, P., Kgaa, M., 2007a. Ficha de Datos de Seguridad Na2HPO4*2H2O. Toxicology 2006, 1–5.

Eur, P., Kgaa, M., 2007b. Ficha de Datos de Seguridad NaCl. Toxicology 2006, 1–5.

Eur, P., Kgaa, M., 2007c. Ficha de Datos de Seguridad Na2S2O8. Toxicology 2006, 1–5. https://doi.org/10.1021/jp000151o

Fernández-Domene, R.M., Roselló-Márquez, G., Sánchez-Tovar, R., Lucas-Granados, B., García-Antón, J., 2019. Photoelectrochemical removal of

chlorfenvinphos by using WO3 nanorods: Influence of annealing temperature and operation pH. Sep. Purif. Technol. 212, 458–464. https://doi.org/10.1016/j.seppur.2018.11.049

Forero, J.-E., Ortiz, O.-P., Rios, F., 2005. Aplicación de procesos de oxidación avanzada como tratamiento de fenol en aguas residuales industriales de refinería. CT&F Ciencia, Tecnol. y Futur. 3, 97–109.

Garcia-Segura, S., Ocon, J.D., Chong, M.N., 2018. Electrochemical oxidation remediation of real wastewater effluents — A review. Process Saf. Environ. Prot. 113, 48–67. https://doi.org/10.1016/J.PSEP.2017.09.014

Gromboni, C.F., Kamogawa, M.Y., Ferreira, A.G., Nóbrega, J.A., Nogueira, A.R.A., 2007. Microwave-assisted photo-Fenton decomposition of chlorfenvinphos and cypermethrin in residual water. J. Photochem. Photobiol. A Chem. 185, 32–37. https://doi.org/10.1016/J.JPHOTOCHEM.2006.05.005

Heberle, A.N.A., da Silva, S.W., Klauck, C.R., Ferreira, J.Z., Rodrigues, M.A.S., Bernardes, A.M., 2017. Electrochemical enhanced photocatalysis to the 2,4,6 Tribromophenol flame retardant degradation. J. Catal. 351, 136–145. https://doi.org/10.1016/J.JCAT.2017.04.011

Hmani, E., Chaabane Elaoud, S., Samet, Y., Abdelhédi, R., 2009. Electrochemical degradation of waters containing O-Toluidine on PbO2 and BDD anodes. J. Hazard. Mater. 170, 928–933. https://doi.org/10.1016/j.jhazmat.2009.05.058

Huie, R.E., Clifton, C.L., Neta, P., 1991. Electron transfer reaction rates and equilibria of the carbonate and sulfate radical anions. Int. J. Radiat. Appl. Instrumentation. Part C. Radiat. Phys. Chem. 38, 477–481.

https://doi.org/10.1016/1359-0197(91)90065-A
Kituyi, E.N., Wandiga, S.O., Jumba, I.O., 1997. Occurrence of chlorfenvinphos residues in cow's milk sampled at a range of sites in western Kenya. Bull. Environ. Contam. Toxicol. 58, 969–975. https://doi.org/10.1007/s001289900429
Klamerth, N., Gernjak, W., Malato, S., Agüera, A., Lendl, B., 2009. Photo-Fenton decomposition of chlorfenvinphos: Determination of reaction pathway. Water Res. 43, 441–449. https://doi.org/10.1016/j.watres.2008.10.013
Li, S., Bejan, D., McDowell, M.S., Bunce, N.J., 2008. Mixed first and zero order kinetics in the electrooxidation of sulfamethoxazole at a boron-doped diamond (BDD) anode. J. Appl. Electrochem. 38, 151–159. https://doi.org/10.1007/s10800-007-9413-2
Liang, C., Huang, C.-F., Mohanty, N., Kurakalva, R.M., 2008. A rapid spectrophotometric determination of persulfate anion in ISCO. Chemosphere 73, 1540–1543. https://doi.org/10.1016/J.CHEMOSPHERE.2008.08.043
Lipp, L., Pletcher, D., 1997. The preparation and characterization of tin dioxide coated titanium electrodes. Electrochim. Acta 42, 1091–1099.
Liu, L., Zhao, G., Wu, M., Lei, Y., Geng, R., 2009. Electrochemical degradation of chlorobenzene on boron-doped diamond and platinum electrodes. J. Hazard. Mater. 168, 179–186. https://doi.org/10.1016/j.jhazmat.2009.02.004
Ma, P., Ma, H., Sabatino, S., Galia, A., Scialdone, O., 2018. Electrochemical treatment of real wastewater. Part 1: Effluents with low conductivity. Chem.

720 Eng. J. 336, 133–140. https://doi.org/10.1016/J.CEJ.2017.11.046
721 Martínez-Huitle, C.A., Rodrigo, M.A., Sirés, I., Scialdone, O., 2015. Single and
722 Coupled Electrochemical Processes and Reactors for the Abatement of
723 Organic Water Pollutants: A Critical Review. Chem. Rev. 115, 13362–
724 13407. https://doi.org/10.1021/acs.chemrev.5b00361
725 Méndez-Martínez, A.J., Dávila-Jiménez, M.M., Ornelas-Dávila, O., Elizalde-
726 González, M.P., Arroyo-Abad, U., Sirés, I., Brillas, E., 2012.
727 Electrochemical reduction and oxidation pathways for Reactive Black 5 dye
728 using nickel electrodes in divided and undivided cells. Electrochim. Acta 59,
729 140–149. https://doi.org/10.1016/j.electacta.2011.10.047
730 Mora-Gómez, J., García-Gabaldón, M., Carrillo-Abad, J., Montañés, M.T.,
731 Mestre, S., Pérez-Herranz, V., 2020. Influence of the reactor configuration
732 and the supporting electrolyte concentration on the electrochemical
733 oxidation of Atenolol using BDD and SnO<inf>2</inf> ceramic electrodes.
734 Sep. Purif. Technol. 241. https://doi.org/10.1016/j.seppur.2020.116684
735 Mora-Gómez, J., García-Gabaldón, M., Ortega, E., Sánchez-Rivera, M.-J.,
736 Mestre, S., Pérez-Herranz, V., 2018. Evaluation of new ceramic electrodes
737 based on Sb-doped SnO2 for the removal of emerging compounds present
738 in wastewater. Ceram. Int. 44, 2216–2222.
739 https://doi.org/10.1016/J.CERAMINT.2017.10.178
740 Mora-Gómez, J., Ortega, E., Mestre, S., Pérez-Herranz, V., García-Gabaldón,
741 M., 2019. Electrochemical degradation of norfloxacin using BDD and new
742 Sb-doped SnO2 ceramic anodes in an electrochemical reactor in the
743 presence and absence of a cation-exchange membrane. Sep. Purif.
744 Technol. 208, 68–75. https://doi.org/10.1016/J.SEPPUR.2018.05.017

745 Moreira, F.C., Boaventura, R.A.R., Brillas, E., Vilar, V.J.P., 2017.
746 Electrochemical advanced oxidation processes : A review on their
747 application to synthetic and real wastewaters. Appl. Catal. B, Environ. 202,
748 217–261. https://doi.org/10.1016/j.apcatb.2016.08.037
749 Murugananthan, M., Latha, S.S., Raju, G.B., Yoshihara, S., 2011. Role of
750 electrolyte on anodic mineralization of atenolol at boron doped diamond
751 and Pt electrodes. Sep. Purif. Technol. 79, 56–62.
752 https://doi.org/10.1016/j.seppur.2011.03.011
753 Oliveira, C., Alves, A., Madeira, L.M., 2014. Treatment of water networks
754 (waters and deposits) contaminated with chlorfenvinphos by oxidation with
755 Fenton's reagent. Chem. Eng. J. 241, 190–199.
756 https://doi.org/10.1016/J.CEJ.2013.12.026
757 Olmez-Hanci, T., Arslan-Alaton, I., 2013. Comparison of sulfate and hydroxyl
758 radical based advanced oxidation of phenol. Chem. Eng. J. 224, 10–16.
759 https://doi.org/10.1016/j.cej.2012.11.007
760 Oturan, N., Trajkovska, S., Oturan, M.A., Couderchet, M., Aaron, J.-J., 2008.
761 Study of the toxicity of diuron and its metabolites formed in aqueous
762 medium during application of the electrochemical advanced oxidation
763 process "electro-Fenton." Chemosphere 73, 1550–1556.
764 https://doi.org/10.1016/J.CHEMOSPHERE.2008.07.082
765 Oturan, N., Wu, J., Zhang, H., Sharma, V.K., Oturan, M.A., 2013.
766 Electrocatalytic destruction of the antibiotic tetracycline in aqueous medium
767 by electrochemical advanced oxidation processes: Effect of electrode
768 materials. Appl. Catal. B Environ. 140–141, 92–97.
769 https://doi.org/10.1016/j.apcatb.2013.03.035

770 Özcan, A., Atılır Özcan, A., Demirci, Y., 2016. Evaluation of mineralization
771 kinetics and pathway of norfloxacin removal from water by electro-Fenton
772 treatment. Chem. Eng. J. 304, 518–526.
773 https://doi.org/10.1016/J.CEJ.2016.06.105
774 Özcan, A.A., Özcan, A., 2018. Investigation of applicability of Electro-Fenton
775 method for the mineralization of naphthol blue black in water.
776 Chemosphere 202, 618–625.
777 https://doi.org/10.1016/j.chemosphere.2018.03.125
778 Radjenović, J., Farré, M.J., Mu, Y., Gernjak, W., Keller, J., 2012. Reductive
779 electrochemical remediation of emerging and regulated disinfection
780 byproducts. Water Res. 46, 1705–1714.
781 https://doi.org/10.1016/j.watres.2011.12.042
782 Rickwood, C.J., Galloway, T.S., 2004. Acetylcholinesterase inhibition as a
783 biomarker of adverse effect: A study of Mytilus edulis exposed to the
784 priority pollutant chlorfenvinphos. Aquat. Toxicol. 67, 45–56.
785 https://doi.org/10.1016/j.aquatox.2003.11.004
786 Rojas, R., Morillo, J., Usero, J., Vanderlinden, E., El Bakouri, H., 2015.
787 Adsorption study of low-cost and locally available organic substances and a
788 soil to remove pesticides from aqueous solutions. J. Hydrol. 520, 461–472.
789 https://doi.org/10.1016/j.jhydrol.2014.10.046
790 Roots, R., Okada, S., 1975. Estimation of Life Times and Diffusion Distances of
791 Radicals Involved in X-Ray-Induced DNA Strand Breaks or Killing of
792 Mammalian Cells. Radiat. Res. 64, 306–320.
793 Roselló-Márquez, G., Fernández-Domene, R.M., Sánchez-Tovar, R., García-
794 Carrión, S., Lucas-Granados, B., García-Antón, J., 2019.

795 Photoelectrocatalyzed degradation of a pesticides mixture solution
796 (chlorfenvinphos and bromacil) by WO3 nanosheets. Sci. Total Environ.
797 674, 88–95. https://doi.org/10.1016/J.SCITOTENV.2019.04.150
798 Ruíz-Delgado, A., Roccamante, M.A., Oller, I., Agüera, A., Malato, S., 2019.
799 Natural chelating agents from olive mill wastewater to enable photo-
800 Fenton-like reactions at natural pH. Catal. Today 328, 281–285.
801 https://doi.org/10.1016/J.CATTOD.2018.10.051
802 Szatkowska, B., Kwiatkowska, M., Michałowicz, J., Sicińska, P., Huras, B.,
803 Bukowska, B., 2012. Impact of chlorfenvinphos, an organophosphate
804 insecticide on human blood mononuclear cells (in vitro). Pestic. Biochem.
805 Physiol. 102, 175–181. https://doi.org/10.1016/J.PESTBP.2012.01.001
806 Wang, Y., Shen, C., Zhang, M., Zhang, B.-T., Yu, Y.-G., 2016. The
807 electrochemical degradation of ciprofloxacin using a SnO2 -Sb/Ti anode:
808 Influencing factors, reaction pathways and energy demand. Chem. Eng. J.
809 296, 79–89. https://doi.org/10.1016/j.cej.2016.03.093
810 Zhang, C., Du, X., Zhang, Z., Fu, D., 2015. The peculiar roles of sulfate
811 electrolytes in BDD anode cells. J. Electrochem. Soc. 162, E85–E89.
812 Zhong, C., Wei, K., Han, W., Wang, L., Sun, X., Li, J., 2013. Electrochemical
813 degradation of tricyclazole in aqueous solution using Ti/SnO2-Sb/PbO2
814 anode. J. Electroanal. Chem. 705, 68–74.
815 https://doi.org/10.1016/j.jelechem.2013.07.027
816
817
818
819